Leak Detection and Isolation in Pressurized Water Pipe Networks using Interval LPV Models

Jorge Vento and Vicenç Puig

Advanced Control Systems Group, Universitat Politècnica de Catalunya, Pau Gargallo, 5, 08028 Barcelona, Spain. (e-mail: vicenc.puig@upc.edu)

Abstract: In this paper, a leak detection and isolation methodology in pressurized water pipe networks is proposed. The methodology is based on computing residuals which are obtained comparing measured pressures (heads) in selected points of the network and their estimated values by means of an interval *Linear Parameter Varying* (LPV) model. The structure of the LPV models is obtained from the non-linear mathematical model of the network. The proposed detection method uses interval LPV models to obtain uncertainty intervals for the estimated heads that allow to indicate when a leak appears in the water network. The isolation task employs an algorithm based on the residual fault sensitivity analysis. Finally, a typical water pipe network is employed to validate the proposed methodology. This network is simulated using EPANET software. Parameters of LPV models and their uncertainty bounded by intervals are estimated from data coming from this simulator. Several leak scenarios allow to assess the effectiveness of the proposed approach.

Keywords: Leak Detection, Fault Isolation, Linear Parameter Varying Model, Sensitivity Matrix.

1. INTRODUCTION

Water system networks are used to supply water for industrial and domestic use. Those systems include sources, treatment works and networks, together with pump stations and reservoirs. They also contain pipes, control valves and water consumers (nodes). Moreover, water systems networks are large-scale systems. Normally, leaks are present in the water consumers or nodes. Therefore, leak detection and isolation methods must be employed to localize leakage in the water distribution system. Model-based leak detection techniques based on the pressure measurements and sensitivity analysis of nodes in a network when a leak is present in a node have been studied (Perez et al., 2009). These techniques are based on the use of the non-linear model of the network. However, the parameter estimation of this model is not an easy task (Brdys and Ulanicki, 1994). This is why this paper proposes alternatively to use a non-linear model with LPV structure whose parameters can be more easily estimated using least-squares algorithms as the one proposed by Bamieh and Giarré (2002), among others.

Linear Parameter Varying (LPV) models have recently attracted the attention of the FDI research community. Such models can be used efficiently to represent some non-linear systems (Shamma and Cloutier, 1993). This has motivated some researchers from the FDI community to develop model-based methods using LPV models (see Bokor et al. (2002), among others). But even with the use of LPV models, modeling errors are inevitable in complex engineering systems. So, in order to increase reliability and performance of model-based fault detection, the development of robust fault detection algorithms should be addressed. The robustness of a fault detection system means that it must be only sensitive to faults, even in the presence of model-reality differences Chen and Patton (1999). One of the approaches to robustness, known as *passive*, is based on enhancing the robustness of the fault detection system at the decision-making stage. The aim with the passive approach is usually to determine, given a set of models, if there is any member in the set that can explain the measurements. A common approach to this problem is to propagate the model uncertainty to the alarm limits of the residuals. When the residuals are outside of the alarm limits, it is argued that model uncertainty alone can not explain the residual and therefore a fault must have occurred. This approach has the drawback that faults that produce a residual deviation smaller than the residual uncertainty due to parameter uncertainty will not be detected.

The typical fault isolation approach proposed in the FDI community uses a set of binary detection tests to compose the observed fault signature. When applying this methodology to leak isolation, since they may exhibit symptoms with different sensitivities, the use of binary codification of the residual produces loss of information (Puig et al., 2005). It is possible to use other additional information associated with the relationship between the residuals and faults, as the residual fault sensitivity, to improve the isolation results (Meseguer et al., 2006).

The innovation of this paper is to present a new leak detection and isolation method for water distribution systems that can be described by LPV models. The fault detection methodology is based on comparing on-line the real system behavior of the monitored system obtained by means of sensors with the estimated behavior using an *LPV interval model*. In the case of a significant discrepancy (residual) is detected between the LPV model and the measurements obtained by the sensors, the existence of a fault is assumed. Due to the effect of the uncertain parameters, the outputs of LPV models are bounded by an interval to avoid false alarms in the detection module. Analyzing in real-time how the faults affect to the residuals using the residual fault sensitivity, it is possible, to isolate the leaks, and even in some cases, it is also possible to determine its magnitude.

The structure of this paper is the following: Section 2 presents the modelling principles of water distribution networks and how to obtain LPV models to represent their dynamics. In Section 3, the leak detection methodology is presented while Section 4 presents the leak isolation and estimation methodology using sensitivity analysis. Finally, in Section 5, an application case study based on an hypothetical water distribution network is used to assess the validity of the proposed approach.

2. MODELLING WATER DISTRIBUTION NETWORKS USING LPV MODELS

2.1 Physical modelling principles

The physical components that constitute a water distribution system are given by a set of pipes, pumps and control valves connected by means of nodes that represent junctions with or without demands and also tanks and reservoirs (Brdys and Ulanicki, 1994). Junctions are points in the network where pipes are joint and where water enters or leaves the network. The reservoirs are nodes that represent an infinite external source to the network, for example, rivers, lakes, groundwater aquifers, and also input points to other system. The tanks are nodes with storage capacity, where the volume of stored water can vary with time.

The pipes transport water from one point in the network to another. Flow direction is always from the end at higher hydraulic head (pressure) to at lower head. The hydraulic head lost by water flowing in a pipe due to friction with the pipes wall can be computed using one of three different formulas: Hazen-Williams (H-W) formula, Darcy-Weisbach (D-W) formula and Chezy-Manning formula(C-M)(Brdys and Ulanicki, 1994). The first formula can be only employed in a pipe for water as liquid and was developed only for turbulent flow. The second formula is applied over all flow regimens and to all liquids and the third formula is used for pipe with long diameter. All these formulas employ the following equation to compute headloss between the start and the end node of the pipe:

$$h_i - h_j = R_{ij} {q_{ij}}^a \tag{1}$$

where: h_i is the pressure at the node i, h_j is the pressure at the node j, R_{ij} is the resistance coefficient, q_{ij} is the flow rate through the pipe, and a is the flow exponent.

The pumps supplies energy to a fluid to raise its hydraulic head. The pumps commonly employed are the centrifuge pumps which contain a rotative system that impulse the water. The valves are used to control the flow or pressure between two parts of the network at a specific point. The valves are classified according to the function that perform.

In each node, the flow continuity law must be fulfilled indicating that sum of flows in a node must be zero, in equation 2 d_i is negative because the demand goes out of the node and q_{ij} are the flows that go into or go out of the node.

$$\sum (q_{ij} - d_i) = 0 \tag{2}$$

The set of equations that describes the water network dynamics can be represented as nodes head function. Solving equation (1) with respect q_{ij} the following flow expression (see equation 3) is obtained

$$q_{ij} = \sqrt[a]{\frac{h_i - h_j}{R_{ij}}} \tag{3}$$

Then, the set of equations that represent the water network dynamic is obtained by replacing Eq. (3) in Eq. (2). This set of equations is non-linear since $a \neq 1$ and can not be solved analytically to obtain the node heads, but instead numerical methods should be used. This non-linearity also makes difficult to estimate the parameters of the network (as, f.e. the pipe resistances). For all these reasons, the non-linear model of the network is not very useful for FDI purposes.

2.2 LPV models

In this paper, is alternatively proposed a linear parametric varying (LPV) model of the water network. LPV models consist of a linear lumped parameters in which the parameters are not constant and depend on system state and/or operating point. There are several ways to obtain an LPV model (Shamma and Cloutier, 1993)(Nelles, 2000)(Bamieh and Giarré, 2002). Here, the LPV model structure of the water distribution network is obtained using physical modeling and Taylor linearisation around a generic operating point Shamma and Cloutier (1993). Parameters are estimated using LPV identification methods (Bamieh and Giarré, 2002). Thus, the water distribution network model can be written using the following LPV representation:

$$\begin{aligned} x(k+1) &= A(\tilde{\vartheta}_k)x(k) + B(\tilde{\vartheta}_k)u_0(k) + F_a(\tilde{\vartheta}_k)f_a(k) \\ y(k) &= C(\tilde{\vartheta}_k)x(k) + D(\tilde{\vartheta}_k)u_0(k) + F_y(\tilde{\vartheta}_k)f_y(k) \end{aligned} \tag{4}$$

where $u_0(t) \in \Re^{n_u}$ is the real system input, $y(t) \in \Re^{n_y}$ is the measured system output, $x(t) \in \Re^{n_x}$ is the state-space vector, $f_a(t) \in \Re^{n_u}$ and $f_y(t) \in \Re^{n_y}$ represents faults in the actuators and system output sensors, respectively. $\tilde{\vartheta}_k{:=}\vartheta(k)$ is the system vector of time-varying parameters of dimension n_ϑ that change with the operating point scheduled by some measured system variables p_k ($p_k{:=}p(k)$) that can be estimated using some known function: $\vartheta_k = f(p_k)$. However, there is still some uncertainty in the estimated values that can be bounded by:

$$\Theta_k = \{\vartheta_k \in \Re^{n_\vartheta} \mid \underline{\vartheta_k} \le \vartheta_k \le \overline{\vartheta_k}\}, \quad \vartheta_k = f(p_k) \tag{5}$$

This set represents the uncertainty about the exact knowledge of real system parameters $\tilde{\vartheta}_k$.

The system (4) describes a model parametrized by a scheduling variable denoted by p_k.

3. LEAKS DETECTION METHODOLOGY

3.1 Input/output form

The system (4) can be expressed in input-output form using the shift operator q^{-1}, assuming zero initial conditions an non-faulty conditions, as follows [1] :

$$\hat{y}(k) = G(q^{-1}, \vartheta_k)u(k) \tag{6}$$

The effect of the uncertain parameters ϑ_k on the temporal response $\hat{y}(k, \vartheta_k)$ can be bounded using an interval satisfying [2] :

$$y(k) \in \left[\underline{\hat{y}}(k), \overline{\hat{y}}(k)\right] \tag{7}$$

[1] In the following, for simplicity and with abuse of notation, transfer functions are used for LPV systems, although computations are performed entirely using the state space representation

[2] In the remainder of the paper, interval bounds for vector variables should be considered component wise.

in a non-faulty case. This interval is computed independently for each output (neglecting couplings between outputs):

$$\underline{\hat{y}}(k) = \min_{\vartheta_k \in \Theta} \left\{ G(q^{-1}, \vartheta_k) u(k) \right\} \tag{8}$$

$$\overline{\hat{y}}(k) = \max_{\vartheta_k \in \Theta} \left\{ G(q^{-1}, \vartheta_k) u(k) \right\} \tag{9}$$

using the zonotope algorithm presented in Guerra et al. (2008).

3.2 Basic adaptive thresholding

Fault detection is based on generating a nominal residual comparing the measurements of physical variables $y(k)$ of the process with their estimation $\hat{y}(k)$ provided by the associated system model:

$$r(k) = y(k) - \hat{y}(k) \tag{10}$$

where $r(k) \in \Re^{n_y}$ is the residual set and $\hat{y}(k)$ is the prediction obtained using the nominal LPV model. According to Gertler (1998), the computational form of the residual generator, obtained using (6), is:

$$r(k) = y(k) - G(q^{-1}, \vartheta_k) u(k) \tag{11}$$

Alternatively, the residual given by (11) can be also expressed in terms of the effects caused by faults using its internal or unknown-input-effect form (Gertler, 1998) as follows:

$$r(k) = G_{f_y}(q^{-1}, \vartheta_k) f_y(k) - G_{f_a}(q^{-1}, \vartheta_k) f_u(k) \tag{12}$$

where $G_{f_y}(q^{-1}, \vartheta_k)$ and $G_{f_a}(q^{-1}, \vartheta_k)$ are the transfer functions that describe the effect of input/output sensors faults in the residual, respectively.

When considering model uncertainty (in this paper, assumed located in parameters), the residual generated by (10) will not be zero, even in a non-faulty scenario. To cope with the parameter uncertainty effect a passive robust approach based on adaptive thresholding can be used (Horak, 1988). Thus, using this passive approach, the effect of parameter uncertainty in the residual $r(k)$ (associated to each system output $y(k)$) is bounded by the interval:

$$r(k) \in [\underline{r}(k), \overline{r}(k)] \tag{13}$$

where:

$$\underline{r}(k) = \underline{\hat{y}}(k) - \hat{y}(k) \text{ and } \overline{r}(k) = \overline{\hat{y}}(k) - \hat{y}(k) \tag{14}$$

being $\hat{y}(k)$ the nominal predicted output, $\underline{\hat{y}}(k)$ and $\overline{\hat{y}}(k)$ the bounds of the predicted output (7). The residual generated by (14) can be expressed in input-output form using (6) as:

$$\underline{r}(k) = \min_{\theta \in \Theta} \left\{ \Delta G(q^{-1}, \vartheta) u(k) \right\} \tag{15}$$

$$\overline{r}(k) = \max_{\theta \in \Theta} \left\{ \Delta G(q^{-1}, \vartheta) u(k) \right\} \tag{16}$$

where:

$$\Delta G(q^{-1}, \vartheta) = G(q^{-1}, \vartheta) - G(q^{-1}, \vartheta_0)$$

being ϑ_0 the nominal parameters.

Then, a fault is indicated if the residuals do not satisfy the relation given by (13), or alternatively, if the measurement is not inside the interval of predicted outputs given by (8)-(9).

4. LEAKS ISOLATION METHODOLOGY

4.1 Fault signature matrix

Fault isolation consists in identifying the faults affecting the system. It is carried out on the basis of fault signatures, (generated by the detection module) and its relation with all the considered faults, $f(k) = \left\{ f_u(k), f_y(k) \right\}$. Robust residual evaluation presented in Section 3.2 allows obtaining a set of *fault signatures* $\phi(k) = [\phi_1(k), \phi_2(k), \ldots, \phi_{ny}(k)]$, where each fault indicator is given by:

$$\phi_i(k) = \begin{cases} 0 & \text{if } r(k) \notin [\underline{r}(k), \overline{r}(k)] \\ 1 & \text{if } r(k) \in [\underline{r}(k), \overline{r}(k)] \end{cases} \tag{17}$$

The standard FDI fault isolation method is based on exploiting the relation defined on the Cartesian product of the sets of considered faults:

$$FSM \subset \phi \times f, \tag{18}$$

where FSM is the theoretical fault signature matrix (Gertler, 1998). One element of such matrix $FSM_{i\ell}$ will be equal to one, if the fault $f_\ell(k)$ is affected by the residual $r_i(k)$. In this case, the value of the fault indicator $\phi_i(k)$ must be equal to one when the fault appears in the monitored system. Otherwise, the element $FSM_{i\ell}$ will be zero.

In leak detection and isolation, the use of the classic binary isolation approach leads to a fault signature matrix full of ones that makes impossible to isolate leaks. This is why in this paper the use use of information provided by the *fault residual sensitivity* is proposed in order to increase leak isolability.

4.2 Leak sensitivity analysis

Since the activation of a residual can be caused by different leaks to distinguish one leak from the others a deep analysis of the residual should be performed. This analysis can be done by means of the *residual fault sensitivity* introduced by (Gertler, 1998) as follows:

$$S_f = \frac{\partial r}{\partial f} \tag{19}$$

that leads to a transfer function that describes the effect on the residual, r, of a given fault f. The expression of residual sensitivities is obtained using the residual internal form given by (12). Thus, the residual (12) can be re-written as follows:

$$r(k) = S_{f_y}(q^{-1}, \tilde{\vartheta}_k) f_y(k) + S_{f_u}(q^{-1}, \tilde{\vartheta}_k) f_u(k) \tag{20}$$

where $S_{f_y}(q^{-1}, \tilde{\vartheta}_k) = G_{f_y}(q^{-1}, \tilde{\vartheta}_k)$ is the sensitivity of the output sensor fault and $S_{f_u}(q^{-1}, \tilde{\vartheta}_k) = -G_{f_u}(q^{-1}, \tilde{\vartheta}_k)$ is the sensitivity of the actuator fault.

Notice that the sensitivity changes with the operating point parametrized by scheduling variable p_k as the LPV system (4).

4.3 Fault isolation and estimation methodology

Figure 1 shows the scheme of the whole leak detection and isolation algorithm proposed in this paper. The detection module has been already explained in Section 3. The result of this module applied to the residual $r(k)$ produces an *observed fault signature* $\phi(k)$. The observed fault signature is then supplied to the fault isolation module that will try to isolate and estimate the leak.

The proposed isolation approach makes use of the fault estimation provided the residual fault sensitivity (19). More precisely, assuming that $\left(S_f(q^{-1}, \tilde{\vartheta}_k)\right)^{-1}$ exists [3], the expression of the fault estimation is given by:

$$\hat{f}_{\varrho,\ell}(k) = \left(S_{f_{\varrho,\ell}}(q^{-1}, \tilde{\vartheta}_k)\right)^{-1} r_i(k) \tag{21}$$

where $i \in [1, \ldots, n_y]$ and being $\hat{f}_{\varrho,\ell} = \left\{\hat{f}_{y,\ell}, \hat{f}_{u,\ell}\right\}$, $\forall\ \ell \in [1, \ldots, n_y, 1, \ldots, n_u]$. This relation considers the influence of each fault $f(k)$ on the each residual $r(k)$.

Using the fault estimation (21), a new *FSM* matrix (called *fault signature matrix FSMest*) can be defined as shown in Table 1. This fault signature matrix is evaluated at every time instant.

$\hat{f}_{\varrho,\ell}$	$f_{y,1}$	$\cdots$	f_{y,n_y}	$f_{u,1}$	$\cdots$	f_{u,n_u}
$r_1(k)$	$\hat{f}_{r_1\, f_{y,1}}$	$\cdots$	$\hat{f}_{r_1\, f_{y,n_y}}$	$\hat{f}_{r_1\, f_{u,1}}$	$\cdots$	$\hat{f}_{r_1\, f_{u,n_u}}$
$r_2(k)$	$\hat{f}_{r_2\, f_{y,1}}$	$\cdots$	$\hat{f}_{r_2\, f_{y,n_y}}$	$\hat{f}_{r_2\, f_{u,1}}$	$\cdots$	$\hat{f}_{r_2\, f_{u,n_u}}$
$\vdots$	$\vdots$	$\ddots$	$\vdots$	$\vdots$	$\ddots$	$\vdots$
$r_{n_y}(k)$	$\hat{f}_{r_{n_y}\, f_{y,1}}$	$\cdots$	$\hat{f}_{r_{n_y}\, f_{y,n_y}}$	$\hat{f}_{r_{n_y}\, f_{u,1}}$	$\cdots$	$\hat{f}_{r_{n_y}\, f_{u,n_u}}$

Table 1. Fault signature matrix based on the fault estimation (*FSMest*) with respect to $r_i(k)$

Each fault hypothesis corresponds to each ℓ^{th}-column of *FSMest* matrix of Table 1. The fault hypothesis corresponding to ℓ^{th}-column is accepted if all the fault estimation values are equal. More precisely, assuming that the system is just affected by one fault $f(k)$ at a time t_0, the isolation process is done by finding the fault that presents a fault estimation with a minimum distance with respect to the average of fault estimation hypothesis being postulated as a diagnosed fault:

$$\min\left\{d_{f_{y,1}}, \ldots, d_{y,n_y}, d_{f_{u,1}}, \ldots, d_{u,n_u}\right\} \tag{22}$$

where the distance is calculated using the Euclidean distance between vectors:

$$d_{f_{\varrho,\ell}} = \sqrt{\left(\hat{f}_{r_1\, f_{\varrho,\ell}}(k) - \hat{f}^{\,m}_{f_{\varrho,\ell}}(k)\right)^2 + \cdots + \left(\hat{f}_{r_{ny}\, f_{\varrho,\ell}}(k) - \hat{f}^{\,m}_{f_{\varrho,\ell}}(k)\right)^2}\, svf_{\varrho,\ell} \tag{23}$$

where:

$$\hat{f}^{\,m}_{f_{\varrho,\ell}}(k) = \frac{\sum_{i=1}^{n_y} \hat{f}_{r_i\, f_{\varrho,\ell}}(k)}{n_y} \quad \text{and} \quad svf_{\varrho,\ell} = \begin{cases} \infty & if FSM \neq r(k) \\ 1 & if FSM = r(k) \end{cases}$$

for $f_{\varrho,\ell} = \left\{f_{y,\ell}, f_{u,\ell}\right\}$, $\forall\ \ell \in [1, \ldots, n_y, 1, \ldots, n_u]$.

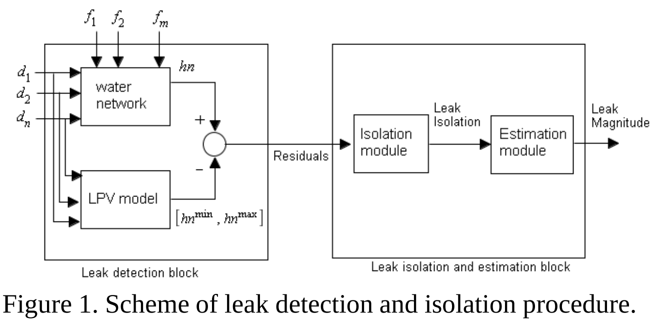

Figure 1. Scheme of leak detection and isolation procedure.

5. APPLICATION CASE STUDY

5.1 Description

The application case study is based on the water distribution network presented in Fig. 2. In this particular case, the water network is composed by the following elements: Two reservoirs, three pipes and two nodes with demands d_1 and d_2 expressed in $\frac{m^3}{s}$. Head sensors (h_{n1} and h_{n2}) (expressed in m) are located in the two nodes. The possible leaks are f_1 and f_2 are also located in the nodes. The pipe resistance coefficients R_1, R_2 and R_3 in the H-W formula (1) are given by $R = \frac{1.2216e10*L}{C^a*D^{4.87}}$ where L is the pipe length in meters (m), D is the pipe diameter in millimeters (mm) and a is flow exponent ($a = 1.852$). The pipes length are $L_1 = L_2 = 1000m$ and $L_3 = 2000m$ respectively and the diameters is the same in all pipes $D_1 = D_2 = D_3 = 200mm$

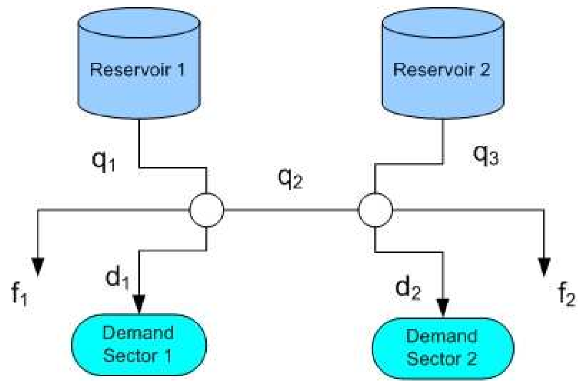

Figure 2. Water network proposed as case study

5.2 LPV modelling

Applying the flow equation (2) to the network under study, the set of equations that describe the flow behaviour is obtained:

$$q_1 + q_2 - d_1 - f_1 = 0 \tag{24}$$

$$q_3 - q_2 - d_2 - f_2 = 0 \tag{25}$$

Analogously, the application of the pressure equation (3) to the case study network leads to the following set of equations:

$$q_1 = \left(-\frac{-h_{d1} + h_{n1}}{R_1}\right)^{a^{-1}} \tag{26}$$

$$q_2 = \left(-\frac{-h_{n2} + h_{n1}}{R_2}\right)^{a^{-1}} \tag{27}$$

$$q_3 = \left(-\frac{-h_{d2} + h_{n2}}{R_3}\right)^{a^{-1}} \tag{28}$$

Finally, the complete non-linear model of the network is obtained by substituting equations (26), (27) and (28) in equations (24) and (25):

$$F_1 = \left(\frac{h_{d1} - h_{n1}}{R_1}\right)^{a^{-1}} + \left(\frac{h_{n2} - h_{n1}}{R_2}\right)^{a^{-1}} - d_1 - f_1 = 0 \tag{29}$$

$$F_2 = \left(\frac{h_{d2} - h_{n2}}{R_3}\right)^{a^{-1}} - \left(\frac{h_{n2} - h_{n1}}{R_2}\right)^{a^{-1}} - d_2 - f_2 = 0 \tag{30}$$

This model is used to develop a high-fidelity simulator of this water network using EPANET software.

[3] If $\left(S_f(q^{-1}, \tilde{\vartheta}_k)\right)^{-1}$ is non-square and can be tackled using the left pseudo-inverse

5.3 LPV identification

To obtain the structure of the LPV model of this network, the non-linear model (29) is linearized around the operating point characterized by the head measurements in nodes h^o_{n1} and h^o_{n2}:

$$\begin{bmatrix} \hat{h}_{n1} \\ \hat{h}_{n2} \end{bmatrix} = A_{hn}{}^{-1} \begin{bmatrix} d_1 \\ d_2 \end{bmatrix} + A_{hn}{}^{-1} \begin{bmatrix} F_1(h^o_{n1}, h^o_{n2}) \\ F_2(h^o_{n1}, h^o_{n2}) \end{bmatrix} + \begin{bmatrix} h^o_{n1} \\ h^o_{n2} \end{bmatrix} \qquad (31)$$

where:

$$A_{hn} = \begin{bmatrix} -\frac{\left(\frac{hd_1-h^o_{n1}}{R_1}\right)^{\frac{1}{a}-1}}{aR_1} - \frac{\left(\frac{h^o_{n2}-h^o_{n1}}{R_2}\right)^{\frac{1}{a}-1}}{aR_2} & \frac{\left(\frac{h^o_{n2}-h^o_{n1}}{R_2}\right)^{\frac{1}{a}-1}}{aR_2} \\ \frac{\left(\frac{h^o_{n2}-h^o_{n1}}{R_2}\right)^{\frac{1}{a}-1}}{aR_2} & -\frac{\left(\frac{h_{d2}-h^o_{n2}}{R_3}\right)^{\frac{1}{a}-1}}{aR_3} - \frac{\left(\frac{h^o_{n2}-h^o_{n1}}{R_2}\right)^{\frac{1}{a}-1}}{aR_2} \end{bmatrix}$$

Notice from Eq. (31) that parameters vary with nodes head. But according to Eqs. (29) and (30), the nodes head is fixed by the demands. Thus, it means that LPV model (31) can alternatively be rewritten as follows:

$$\begin{aligned} \hat{h}_{n1} &= a_{11}(d_1,d_2)d_1 + a_{12}(d_1,d_2)d_2 + a_{13}(d_1,d_2) \\ \hat{h}_{n2} &= a_{21}(d_1,d_2)d_1 + a_{22}(d_1,d_2)d_2 + a_{23}(d_1,d_2) \end{aligned} \qquad (32)$$

Parameterizing the parameter dependence of this model with the demand as follows

$$a_{ij} = \alpha_{ij}d_1 + \beta_{ij}d_2 + \gamma_{ij} \qquad (33)$$

and using the LPV parameter estimation algorithm proposed by Bamieh and Giarré (2002) to a set of head/demand data registered in the netowrk in a non-leak scenario, the parameters α_{ij}, β_{ij} and γ_{ij} are obtained. Table 2 shows the numeric values of these parameters. Figure 3 presents graphically the values of these parameters in function of the demands.

α_{11}	-0.0105	α_{21}	-0.0086
β_{11}	-0.0027	β_{21}	-0.0050
γ_{11}	0.0006	γ_{21}	0.0033
α_{12}	-0.0027	α_{22}	-0.0050
β_{12}	-0.0047	β_{22}	-0.0016
γ_{12}	-0.0236	γ_{22}	-0.0290
α_{13}	0.0543	α_{23}	0.0498
β_{13}	0.0229	β_{23}	0.0274
γ_{13}	14.8658	γ_{23}	14.8713

Table 2. Estimated α_{ij}, β_{ij} and γ_{ij} parameters corresponding to LPV parameter $a_{ij} = \alpha_{ij}d_1 + \beta_{ij}d_2 + \gamma_{ij}$

Once the nominal LPV model has been estimated, parametric modelling uncertainty λ_{ij} for each LPV parameter a_{ij} will be bounded using intervals such that

$$a_{ij} \in \left[a^0_{ij}(d_1,d_2) - \lambda_{ij}, a^0_i(d_1,d_2) + \lambda_{ij}\right]. \qquad (34)$$

This uncertainty will be bounded using the algorithm proposed by Ploix et al. (1999) that guarantees that all registered input/output data from the system in non-faulty scenarios will be included in the interval model. As a result of application of this algorithm $\lambda_{ij} = 0.007$ for all parameters.

Figure 4 presents the maximum (blue) and minimum (red) prediction bounds for node heads provided by the LPV model (31). It can be noticed that the real node heads are inside the minimum and maximum prediction bounds.

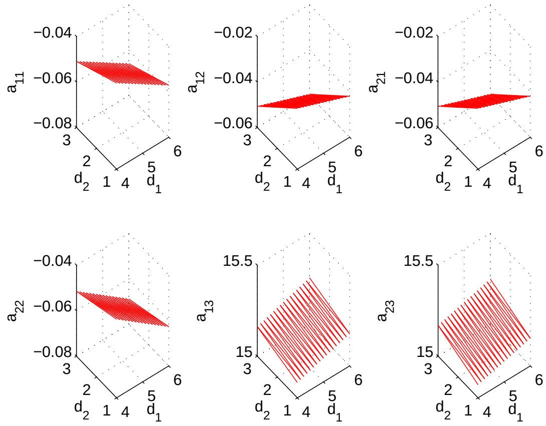

Figure 3. LPV parameters variation with the demands

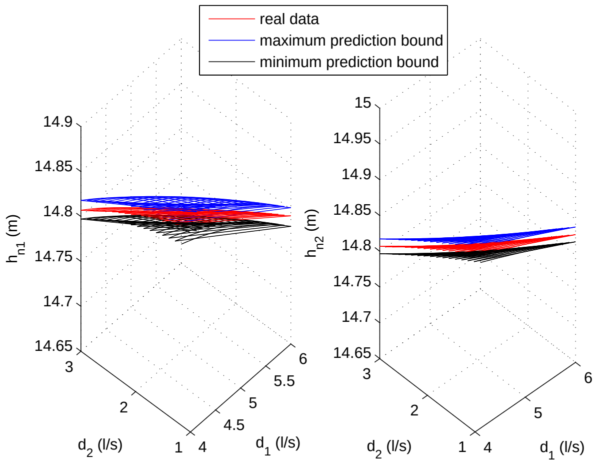

Figure 4. Variation of head prediction bounds with demands.

5.4 Leak detection and isolation implementation

Using the LPV model (32) with the parameters and uncertainty estimated above, the fault detection procedure described by Section 3 is implemented considering the following residuals

$$\begin{aligned} r_{n1} &= h_{n1} - \hat{h}_{n1} \\ r_{n2} &= h_{n2} - \hat{h}_{n2} \end{aligned} \qquad (35)$$

where $\hat{h}_{n1}$ and $\hat{h}_{n2}$ are given by Eq. (32).

Fault isolation procedure is implemented using the fault isolation procedure described by Section 4 and residuals (35). To implement such procedure the effect of leaks is included in the LPV model (32) as follows

$$\begin{aligned} r_{n1} &= a_{11}(d_1,d_2)f_1 + a_{12}(d_1,d_2)f_2 \\ r_{n2} &= a_{21}(d_1,d_2)f_1 + a_{22}(d_1,d_2)f_2 \end{aligned} \qquad (36)$$

that leads to the following leak sensitivity matrix using the fault residual sensitivity definition (19)

$$S(d_1,d_2) = \begin{bmatrix} a_{11}(d_1,d_2) & a_{12}(d_1,d_2) \\ a_{21}(d_1,d_2) & a_{22}(d_1,d_2) \end{bmatrix} \qquad (37)$$

5.5 *Leak isolation and estimation scenarios*

To show the effectiveness of the proposed method two leak scenarios corresponding to leaks appearing in nodes 1 and 2 are considered.

Leak scenario 1. Figure 5 (top plots) shows the evaluation of real head measurements against prediction bounds using the LPV interval model (32) when a leak f_1 is present in the node 1. Notice that the nodes head measurements do not belong to the uncertainty interval once the leak appears. Once the leak is detected, fault isolation and estimation modules isolate and estimate the leak. Figure 7 illustrates the leak isolation result using the rule (22). Figure 5 (bottom plots) also illustrates the leak magnitude estimation using Eq. (21).

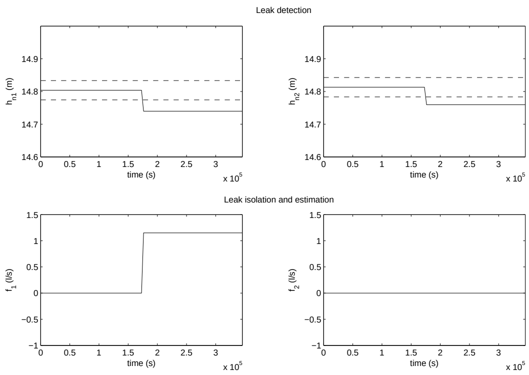

Figure 5. Fault Detection and Estimation in Scenario 1

Fault scenario 2. Figure 6 (top plots) shows the evaluation of the model prediction against prediction bounds when a leak f_2 is present in the node 2. As in the case of fault scenario 2, Figure 7 illustrates the leak isolation result using the rule (22) while Figure 6 (bottom plots) also illustrates the leak magnitude estimation using Eq. (21).

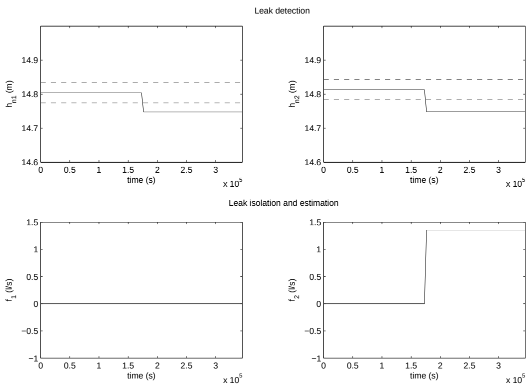

Figure 6. Fault Detection and Estimation in Scenario 2

6. CONCLUSIONS

In this paper, a leak detection and isolation method for water pipe network system described by means of LPV model has been proposed. The leak detection methodology is based on checking if head measurements are inside the prediction bounds provided by a interval LPV model. The leak isolation module has been implemented using fault residual sensitivity analysis. This concept has been used to provide additional information

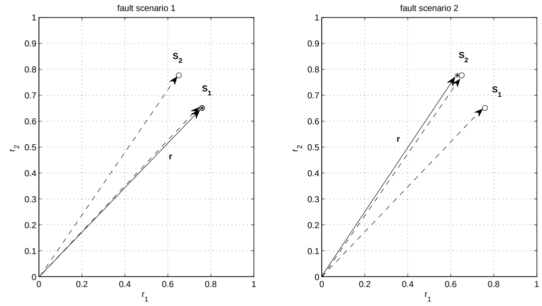

Figure 7. Fault Isolation in Scenario 1 and 2

to the relationship between residuals and leaks. Moreover, it allows obtaining a leak estimation. Satisfactory results are obtained using the water pipe network case study. As a further research, the proposed methodology will be applied in a real network.

7. ACKNOWLEDGMENTS

This work has been partially funded by the grant CICYT DPI2008-01996 of Spanish Ministry of Education.

REFERENCES

B. Bamieh and L. Giarré. Identification of linear parameter varying models. *International Journal Robust Nonlinear Control*, 2(12):841–853, 2002.

J. Bokor, Z. Szabo, and G. Stikkel. Failure detection for quasi LPV systems. *Proceedings of the 41st IEEE Conference on Decision and Control*, 3:3318–3323, 2002.

M. A. Brdys and B. Ulanicki. *Water Systems Structures, Algorithms and Applications*. Prentice Hall, 1994.

J. Chen and R. J. Patton. *Robust model-based fault diagnosis for dynamic systems*. Kluwer Academic Publishers, 1999.

J. Gertler. *Fault Detection and Diagnosis in Engineering Systems*. Marcel Dekker, New York, 1998. ISBN 0824794273.

P. Guerra, V. Puig, and M. Witczak. Robust fault detection with unknown-input interval observers using zonotopes. *Proceedings of the 17th World Congress The International Federation of Automatic Control*, pages 5557–5562, 2008.

D. T. Horak. Failure detection in dynamic systems with modelling errors. *Journal of Guidance, Control, and Dynamics*, 11(6):508–516, 1988.

J. Meseguer, V. Puig, and T. Escobet. Observer gain effect in linear interval observer-based fault detection. *Sixth IFAC Symposium on Fault Detection, Supervision and Safety of Technical Processes*, 6, 2006.

O. Nelles. *Nonlinear System Identification*. Springer, 2000.

R. Perez, V. Puig, and J. Pascual. Leakage detection using pressure sensitivity analysis. *Computing and Control in the Water Industry Conference, Sheffield, UK*, 2009.

S. Ploix, O. Adrot, and J. Ragot. Parameter uncertainty computation in static linear models. *Proceedings of the 38th IEEE Conference on Decision and Control*, 2:1916–1921, 1999.

V. Puig, F. Schmid, J. Quevedo, and B. Pulido. A new fault diagnosis algorithm that improves the integration of fault detection and isolation. *44th IEEE Conference on Decision and Control, and the European Control Conference 2005. Seville, Spain*, pages 3809–3814, 2005.

J.S. Shamma and J.R. Cloutier. Gain scheduled missile autopilot design using linear parameter varying transformations. *AIAA Journal of Guidance, Control, and Dynamics*, 16(2): 256–263, 1993.